



Article

Exploring the Effect of Natural *Ficus benghalensis* Tree Aerial Root Powder on the Mechanical Properties of Basalt-Fiber-Reinforced Polymer Composites

Suhas Yeshwant Nayak, Anupama Hiremath *¹, Gururaj Bolar *², Atharva Sachin Punekar, Shivam Prakash, Hrithik Shetty and Jeppu Pramod Jaideep

Department of Mechanical and Industrial Engineering, Manipal Institute of Technology, Manipal Academy of Higher Education, Manipal 576 104, Karnataka, India; suhas.nayak@manipal.edu (S.Y.N.); atharva.punekar@learner.manipal.edu (A.S.P.); shivam.prakash@learner.manipal.edu (S.P.); hrithik.shetty@learner.manipal.edu (H.S.); jaideep.mitmpl2023@learner.manipal.edu (J.P.J.)

* Correspondence: anupama.hiremath@manipal.edu (A.H.); gururaj.bolar@manipal.edu (G.B.)

Abstract: Banyan aerial root (BAR) powder was prepared from the aerial roots of a Banyan tree to modify epoxy resin using a magnetic stirrer. The modification was performed at different proportions of BAR powder, namely, 2%, 4%, 6%, and 8%, by weight. Composites were fabricated with modified and unmodified resins using a combination of hand lay-up and compression molding processes to evaluate the influence of BAR powders on their mechanical properties. The test results showed that BAR powder incorporation had a positive influence on the mechanical properties of the composites, as an increase in tensile, flexural, and impact strengths was observed, with the highest tensile and flexural properties of 407.81 MPa and 339 MPa, respectively, seen in composites with 4% BAR and the highest impact strength 194.02 kJ/m² observed in the specimen with 6% BAR powder. Though the properties saw a dipping trend at higher weight proportions of the particulate, they were still significantly higher than the properties of laminates prepared with unmodified resin. Gravimetric analysis and Fourier transform infrared spectroscopy (FTIR) on BAR powders confirmed cellulose to be the major constituent, followed by lignin and hemicellulose. A scanning electron microscope was used for studying the failure mechanisms of the laminates.

Keywords: Banyan tree aerial root powder; basalt fiber; epoxy composites; mechanical properties; resin modification



Citation: Nayak, S.Y.; Hiremath, A.; Bolar, G.; Punekar, A.S.; Prakash, S.; Shetty, H.; Jaideep, J.P. Exploring the Effect of Natural *Ficus benghalensis* Tree Aerial Root Powder on the Mechanical Properties of Basalt-Fiber-Reinforced Polymer Composites. *J. Compos. Sci.* **2023**, *7*, 493. <https://doi.org/10.3390/jcs7120493>

Academic Editor: Alessandro Pegoretti

Received: 28 September 2023

Revised: 21 October 2023

Accepted: 6 November 2023

Published: 29 November 2023



Copyright: © 2023 by the authors. Licensee MDPI, Basel, Switzerland. This article is an open access article distributed under the terms and conditions of the Creative Commons Attribution (CC BY) license (<https://creativecommons.org/licenses/by/4.0/>).

1. Introduction

Over the years, there has been a significant surge in the demand and use of composite materials, specifically fiber-reinforced polymer (FRP) composites, which have found applications in practically all types of advanced engineering structures. Composites are made from two or more constituent materials with significantly different properties that remain separate and distinct within the finished structure. Fiber-reinforced polymer (FRP) composites belong to a category of composite materials that comprise a high-performing fiber and a polymer matrix such as epoxy. Polymer composites possess a high strength-to-weight ratio; are resistant against chemicals, weather, wear, and corrosion; and allow flexibility in their design [1]. Therefore, the demand for polymer composites is widely felt in various industries, such as airframes for aerospace vehicles [2], sports equipment [3], personal protective armor [4], marine applications [5], and civil infrastructure [6].

Presently, FRP composites are made using synthetic fibers like glass, carbon, and aramid. Synthetic fibers, a potential reinforcement material in composites, have been used for a long period and have proven their superiority. However, their detrimental effects, such as increased production cost, health hazards, and difficulty in recycling after their useful life, make them a problem in the long run [7]. Thus, there is an increasing demand for

natural alternatives. Natural fibers possess properties like low cost, lightweight, minimal health hazards during processing, and biodegradable characteristics, which make them attractive alternatives to synthetic fibers [8]. Natural fibers can be classified into three categories based on their origin; they may be plant-, animal-, or mineral-based [9].

Mineral-based natural fibers, such as basalt, have attracted a lot of attention not only because of their ecofriendly, nontoxic, and green characteristics, but also owing to their low cost and better mechanical properties and the presence of abundant basalt reserves on Earth [10]. Basalt fiber, commonly also known as a green industrial material, is a high-performing inorganic fiber that is 100% natural and inert. Furthermore, it has also been tested, and it has been proven that it is noncarcinogenic and nontoxic [11]. Apart from being ecofriendly and inexpensive, basalt fibers are easy to process and have high strength, good modulus, improved strain to failure, high temperature resistance, good chemical resistance, high resistance to corrosion, very low thermal conductivity, and excellent stability [12,13]. Furthermore, it has also been found that these properties of basalt fibers are superior to those of carbon fibers and E-glass fibers [14]. Thus, basalt fibers have a wide range of applications and are already being used in industries such as the automotive [15], construction [16], chemical and petrochemical [17], windmill blade [18], and sporting gear [19] industries. These characteristics make basalt fibers an important reinforcement material in polymer composites compared to other natural fibers.

The addition of fillers at an optimum proportion have shown significant improvements in the mechanical, thermal, and tribological properties of composites [20]. Fillers can be either synthetic or natural, based on their origin. Regarding the ecological aspect, researchers are constantly exploring the field of natural fillers. Natural fillers are derived from nature and thus have the additional benefits of being biodegradable, easily available, and inexpensive [21]. Natural fillers, such as rice husk ash [22], sawdust [23], tamarind seed powder [24], eggshell powder [25], coconut coir powder, coconut shell powder [26], seashell powder [27], etc., have been explored. Research involving tamarind seed powder indicated an improvement in the mechanical properties of natural-fiber-reinforced epoxy composites at 7.5 wt.% addition of tamarind seed powder [28]. *Asparagus racemosus* root powder as a filler in a polyvinyl alcohol (PVA) matrix has been reported as a promising material that can be used in wearable electronics that require proper electromagnetic shielding [29]. Efforts are also being made to incorporate natural fillers that pose threats to ecology, such as the root system of a water hyacinth plant. A published report incorporated the ash of the root of water hyacinth along with eggshell powder as fillers in polymer resin [30]. The findings indicated that the developed composites could be successfully used as medium-density particle boards. Natural fillers are also found to be effective flame retardants that can easily replace synthetic flame-retardant fillers. Published research has reported that through the incorporation of the Sirisha tree's bark powder as a filler in a coir fiber/polypropylene composite, the flammability properties of the composite increase [31]. Rice husk, which is an agricultural waste, has been successfully valorized as a filler in various polymer composites. Through additional treatments, rice husk filler use has improved the electrical insulating properties of epoxy-based composites [32]. Natural fillers have also been successfully incorporated not only in thermoset matrices but also in thermoplastic matrices. One such study highlighted that a 20 wt.% coconut-coir-filled high-density polyethylene (HDPE) composite could be successfully injection-molded to produce cloth clips [33].

Such research findings make polymer composites filled with natural fillers a very promising and ever-broadening field of study. Though researchers around the globe have come up with different natural fillers that can enhance the performance of the composite, there are many areas still left unexplored as far as natural fillers are concerned. The Banyan tree, referred to as "*Ficus bengalensis*", is the national tree of India and is widely available in the regions of India and Bangladesh. BARs are a common observation in Banyan trees. These aerial roots are synthesized as fibers and have been studied for their unique properties. It has been reported that the fibers extracted from the aerial roots of the Banyan tree have

an inherent antimicrobial property, which is rarely found in cellulosic fibers [34]. The fibers extracted from the aerial roots of the Banyan tree have been found to have good adhesion with polymer resin, making them good candidate fibers for producing high-performance polymer composites [35,36]. Another research finding indicated that the addition of 4 wt.% graphene powder in 40 wt.% Banyan-fiber-reinforced polymer composites improved the tensile and flexural strength of the hybrid polymer composite [37]. Published research has reported the beneficial effect of graphene powder/Banyan tree aerial root fiber/flax fiber/epoxy in 2%, 19%, 19%, and 60 wt.% proportions, respectively, on the mechanical properties of hybrid composites [38]. However, not much progress has been made until now in studying the effect of aerial roots of the Banyan tree as a natural filler in powder form in polymer resins. The present work focuses on using this novel BAR powder as a microfiller in basalt/epoxy composites. This paper aims to study the effect of BAR powder on the mechanical properties of the composites. Also, an optimum proportion of BAR powder in epoxy resin that shows the highest mechanical properties was identified.

2. Experimental Section

2.1. Materials

Plain woven basalt fiber with an areal density of 380 gsm was procured from Composites Tomorrow, Vadodara, Gujarat, India. The BAR was procured from Banyan trees that were locally available in Manipal, India. Multifunctional epoxy (Lapox A53) and a compatible hardener (K6) (room-temperature-cure system) were procured from Atul Industries, Ahmedabad, Gujarat, India, and were used as a matrix material.

2.2. Preparation of BAR Powder

The BAR powder was prepared from a big individual BAR. The big individual roots were cut into smaller pieces and dried using a hot-air oven at 90 °C for 24 h until no significant change in the weight was observed. The dried samples were then hand-crushed into smaller fibers using a stone crusher and were further powdered in the ball mill. BAR powder was then sieved using a 180 µm diameter opening sieve followed by a 45 µm diameter opening sieve.

2.3. Characterization of BAR

The final composite property depends upon the chemical composition of fibers and fillers and their compatibility with the matrix material. The chemical composition of basalt fiber is well established through various published studies [39]. However, no published study has explored the chemical composition of the novel BAR powder filler. Hence, analyzing the chemical composition of the BAR powder is important to understand the effect of the filler on the mechanical properties of the composite. The chemical constituents of the BAR powder were determined by performing a gravimetric analysis [40]. Constituents like cellulose, hemicellulose, and lignin were quantitatively determined by performing neutral detergent fiber (NDF), acid detergent fiber (ADF), and acid detergent lignin (ADL) procedures. The value obtained from NDF informs us about the hemicellulose, cellulose, lignin, and trace minerals of the powder. NDF provides details about the content of hemicellulose, cellulose, lignin, and minerals, while ADF provides information about the contents of cellulose, lignin, and minerals present in the BAR powder. The total hemicellulose content in the BAR powder was estimated by subtracting the value obtained using ADF from the value obtained using NDF. Similarly, the total cellulose content in the BAR powder was obtained by subtracting the ADF value from the ADL value. The lignin content was obtained through the ADL method. A Fourier transform infrared spectroscopy (FTIR) study was also performed on the BAR powder to understand the presence of specific functional groups in it.

2.4. Fabrication of Composites

A single panel was made using 12 piles of basalt fiber, each of dimensions 290 mm × 260 mm. The epoxy resin was modified by dispersing BAR powder into it using a magnetic stirrer for 40 min at 300 rpm and 70 °C. The BAR powder proportions were chosen to be 2%, 4%, 6%, and 8 wt.% of the resin based on the study from the published literature where researchers observed a decrease in mechanical properties with higher filler proportions [41]. The hardener was then added to the resin just before the hand lay-up was performed (where the ratio of epoxy to hardener was fixed as 10:1). Composite panels were fabricated using hand lay-up and press-molding techniques. The hand lay-up process was performed on an open mold, after which the panel was compressed under a hydraulic press where it was left for 24 h. The required laminates were prepared by keeping the wt.% of the BF constant, whereas the resin content was varied concerning the varying BAR filler wt.% [42–44]. The panel was compressed to a thickness of 2.5 mm using precisely machined shims at a compression factor of 1.4 [45]. After removing the panel from the press mold, it was kept aside for seven days at room temperature as a post-curing step. Using a similar technique, an additional panel without using any fillers was also prepared to evaluate the effect of the BAR powder as a filler on the mechanical properties of the composites. Figure 1 illustrates the fabrication process employed to prepare the required laminates. After fabrication, the panel surface was wiped/cleaned and named as presented in Table 1.

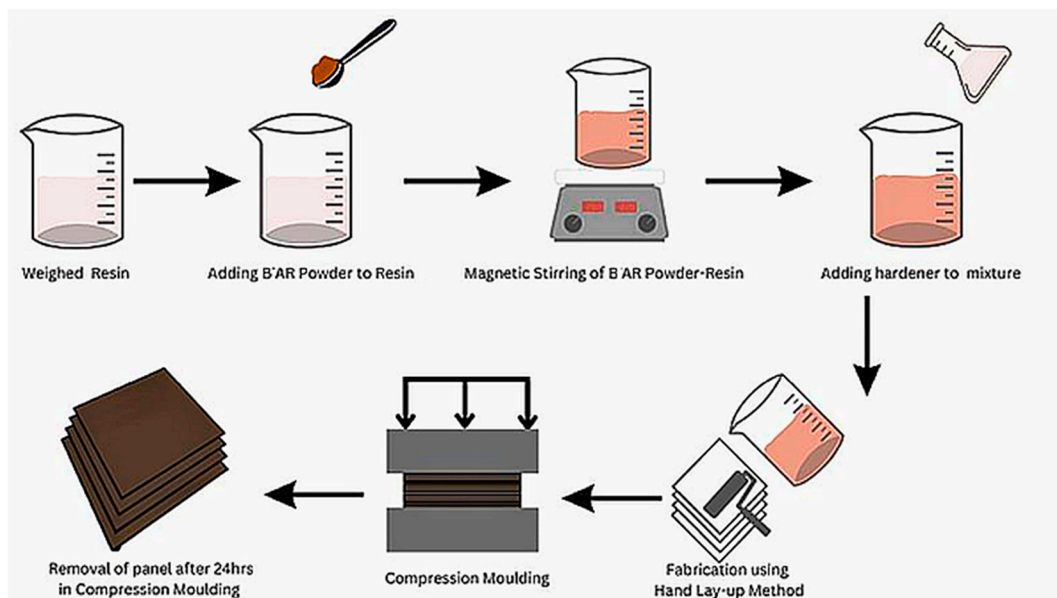


Figure 1. Preparation of the laminates.

Table 1. Designation and compositional details of composites.

Composite Designation	Proportions of Constituents (wt.%)		
	BAR Powder	Epoxy Resin	Basalt Fiber
BEC0	0	50	50
BEC2	2	48	50
BEC4	4	46	50
BEC6	6	44	50
BEC8	8	42	50

2.5. Mechanical Testing of Composites

The composites that were fabricated were tested for a series of mechanical tests which included tensile, flexural, and impact strength tests. The specimens were cut from the composite panels according to the respective standards using an Abrasive Water Jet Machine (AWJM). The tensile test as per ASTM D3039 standard was performed on a Universal Testing Machine (UTM) (Make—MTS; Model—E43) with a constant loading rate of 2 mm/min. The specimen size was 250 mm × 25 mm. The flexural strength test as per the ASTM D7264 standard was performed on a UTM (Make—Zwick Roell, Kennesaw, GA, USA; Model—Z020). The specimen length for the flexural test was 96 mm, with a span length of 80 mm and width of 13 mm. The rate of loading for the flexural tests was 1 mm/min. Impact testing (Charpy) as per the ISO179/1fU standards was performed on an un-notched specimen using a pendulum-type impact testing machine (Make—Zwick Roell, Kennesaw, GA, USA; Model—HIT 50P), and the dimensions of the specimen were 80 mm × 10 mm. A total of fifteen specimens were cut from a composite panel, with five specimens per mechanical test.

2.6. Fracture Analysis through SEM

A scanning electron microscope (SEM) was used to determine the various modes of failure in a composite specimen. Failed samples of the flexural test were coated with gold–palladium via ion sputtering before they were analyzed with the SEM. This coating makes the specimen conductive and avoids its charging due to prolonged exposure to the electron beam. An accelerating voltage of 10 kV under low pressure was used for the analysis.

3. Results and Discussion

3.1. Characterization of BAR

Gravimetric analysis indicated that the BAR powder was composed of approximately 52% cellulose and around 10% hemicellulose, and the lignin content was found to be around 23%. Figure 2 shows the FTIR transmission spectrum of the BAR powder. Table 2 summarizes the observed bond types and the possible compounds present in the BAR powder corresponding to the peaks observed in the FTIR spectrum.

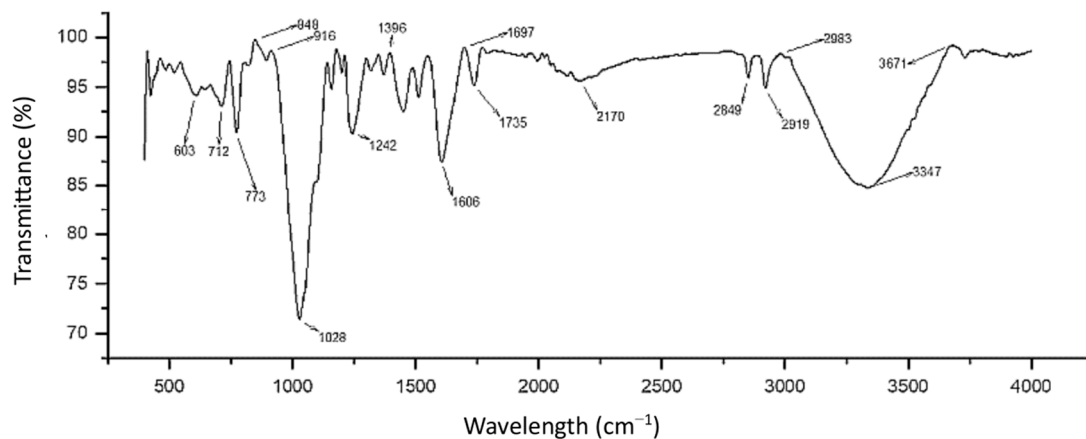


Figure 2. FTIR spectrum of BAR powder.

Table 2. Bond types and possible compounds in BAR powder based on FTIR spectrum.

Wavelength (cm ⁻¹)	Bond and Vibration Type	Possible Compounds
712	C–Cl stretch, C–H “oop”, N–H wag, =C–H bend	Aromatic hydrogen of lignin [46,47]
773	C–Cl stretch, C–H “oop”, N–H wag, =C–H bend	Aromatic hydrogen of lignin [46,47]
1028	C–N stretch, C–O stretch	Alcohol groups of cellulose; aliphatic alcohols and ethers of lignin; pectin [48]

Table 2. Cont.

Wavelength (cm^{-1})	Bond and Vibration Type	Possible Compounds
1242	C–N stretch, C–H wag, C–O stretch,	Alcohol groups of cellulose; aliphatic alcohols and ethers of lignin; pectin
1606	C=O stretch	Lignin
1735	C=O stretch	Carbonyl ester and carboxyl of carboxylic acid of hemicellulose; carbonyl aldehyde or ketone and carboxyl of carboxylic acid of lignin; carboxyl ester of pectin and carbonyl ester of waxes
19	C–H stretch	Aliphatic and alkyl compounds of cellulose; methyl groups of hemicellulose; methoxyl groups of lignin and methylene groups of waxes [48]
3347	N–H stretch, O–H stretch, H-bonded	Hydroxyl group of cellulose, hemicellulose, and waxes; phenolic and aliphatic hydroxyl groups of lignin [49]

Judging from the SEM images of the BAR powder shown in Figure 3, the powder is characterized by an irregular particle shape and varied particle size. All particles exhibited sufficient surface roughness and enhanced crystallinity.

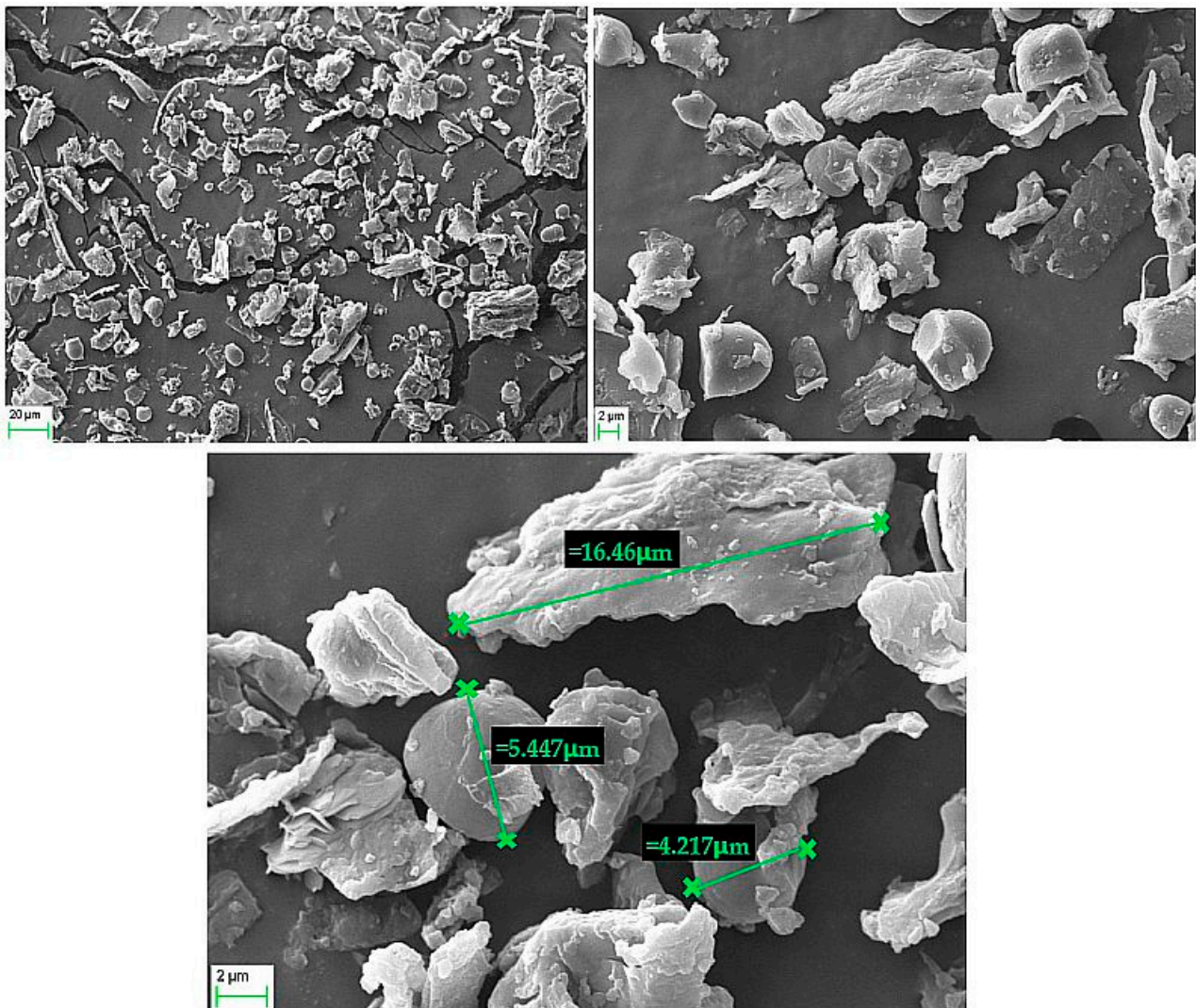


Figure 3. SEM images of BAR powder.

3.2. FTIR Analysis of BEC Laminates

Figure 4 shows the FTIR spectra for the BAR-powder-filled as well as the unfilled BEC laminates. The addition of BAR powder resulted in the generation of additional functional groups, denoted by the presence of absorbance peaks for the BEC2, BEC4, BEC6, and BEC8 laminates in the wavelength range of $800\text{--}1800\text{ cm}^{-1}$, which are absent in the spectrum of the BEC0 laminate. The band at $1000\text{--}1100\text{ cm}^{-1}$ for the BEC2, BEC4, and BEC8 laminates indicates vibrations due to the C–N stretch, which in turn indicates a strong crosslinking reaction [50].

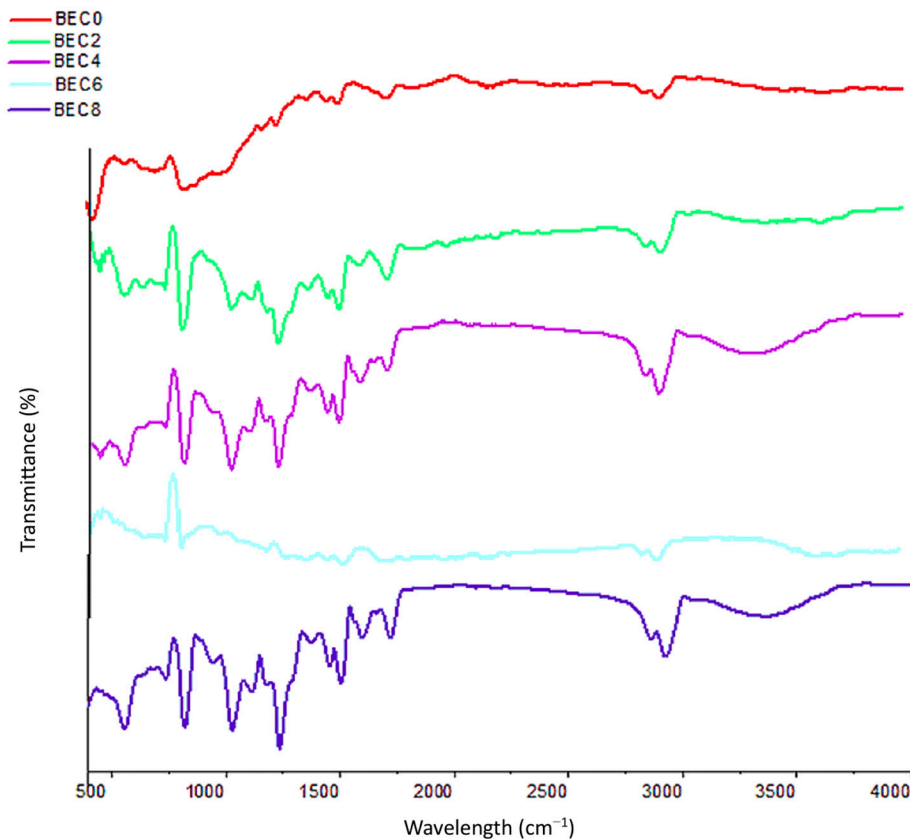


Figure 4. FTIR spectra of BEC laminates.

The presence of absorbance peaks in the wavelength of $2700\text{--}2900\text{ cm}^{-1}$ for the BEC2, BEC4, BEC6, and BEC8 laminates, which are more prominent than in the BEC0 laminate, may be due to the C–H stretch in the aliphatic and alkyl compounds of cellulose, methyl groups of hemicellulose, and methoxyl groups of lignin present in the BAR powder. Broad absorbance peaks in the wavelength range of $3000\text{--}3500\text{ cm}^{-1}$ can be seen for the BEC4 and BEC8 laminates, which are due to the stretching of the hydrogen bonds.

3.3. Mechanical Properties of the Composites

3.3.1. Tensile Strength

The tensile strength of the BEC laminates is shown in Figure 5. The analysis of the results indicates that the tensile strength of the BEC laminates that are fabricated with the inclusion of the BAR powder as filler is high in comparison to that of the BEC0 laminate, which was fabricated without the inclusion of the BAR filler. The maximum tensile strength was found in the BEC4 composite, about 407.81 MPa. When compared with the BEC0 composite, which had a tensile strength of nearly 251.13 MPa, the increase in tensile strength was about 62%. The composites with 2 wt.% BAR, 6 wt.% BAR, and 8 wt.% BAR showed tensile strengths of 307.71 MPa, 328.61 MPa, and 302.48 MPa, respectively, which are about 23%, 31%, and 20% stronger than that of composite BEC0. This indicates that the inclusion of BAR powder as a filler is beneficial for the improvement in the tensile strength of BEC

laminates. This can be attributed to the fact that BAR powder is composed of lignin, which is known to contain several functional groups such as hydroxyls, carboxyl, carbonyl, and methyl [51]. Thus, the BAR powder consists of several active functional reaction sites that can react with the epoxides of the resin and metal ions of the basalt fibers and result in the formation of healthy interfaces between the matrix, filler, and fiber.

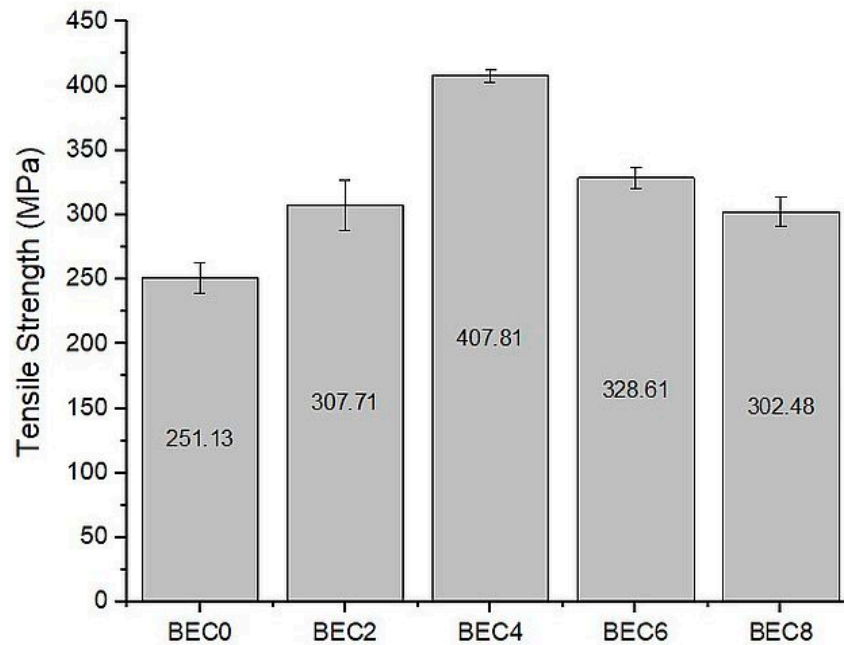


Figure 5. Tensile strength of BEC laminates.

Figure 6 shows the stress–strain curve of the BEC laminates. The analysis of this plot indicates the brittle fracture of all BEC laminates, with fracture occurring between a strain of 5% and 7%. This means that the incorporation of the BAR filler rendered the BEC laminate stiff, thus improving the laminate’s resistance to deformation under the applied loads.

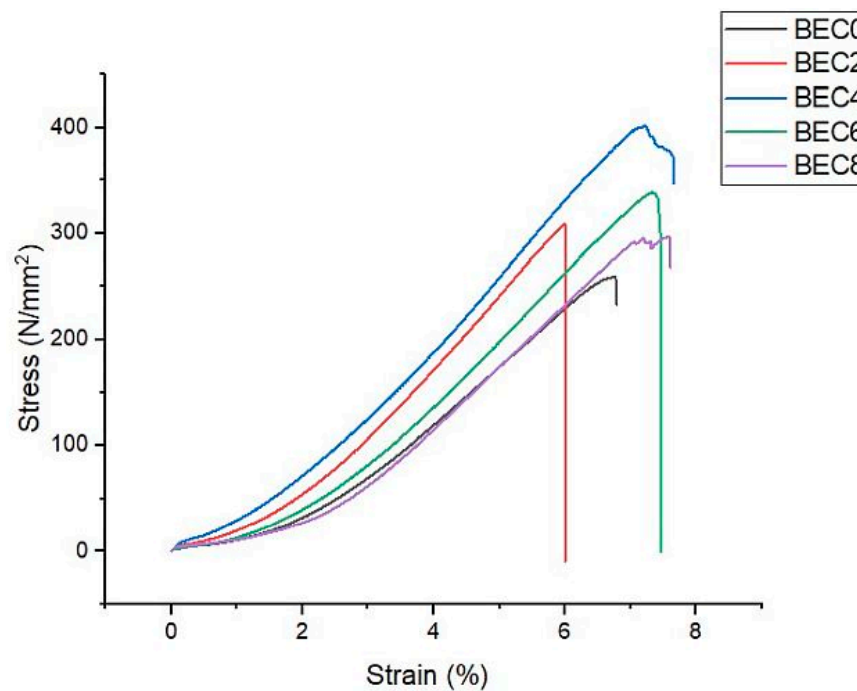


Figure 6. Stress–strain curve of the BEC laminates.

The generation of strong interfaces results in the effective transfer of tensile loads between the various components of the composite and thus results in the improvement of the overall tensile strength of the BEC laminate. The tensile strength increases in the BEC2 laminate and reaches a maximum value in the BEC4 laminate. However, the tensile strength starts to decrease in the BEC6 and BEC8 laminates, indicating that the optimum wt.% of BAR powder is around 4 wt.%, beyond which the addition of the BAR powder does not positively improve the tensile strength of the BEC laminate. At a higher wt.% addition of BAR powder, the resin content is reduced, making the resin solution highly viscous. Thus, the resin's flowability is greatly hampered at a higher wt.% loading of the BAR powder filler. Under such circumstances, the basalt fibers are sparsely coated with the BAR-powder-filled resin. At such reduced wettability, there is a lack of generation of stronger interfaces between the resin and the fibers. Due to this, the applied tensile loads cannot be transferred effectively and efficiently from the weaker resin matrix to the stiffer fibers. Thus, at a higher wt.% addition of BAR powder, the tensile strength of the BEC laminates is reduced.

3.3.2. Flexural Strength

The flexural strength and modulus of the BEC laminates are presented in Figure 7. In Figure 7, an increasing trend in the flexural strength and moduli is observed for all of the BEC laminates which were fabricated with the inclusion of BAR powder, in comparison with the BEC0 laminate, which did not have BAR powder in it. The maximum flexural strength was observed in the BEC4 composite, which was about 339 MPa. When compared with the BEC0 composite, which had a flexural strength of nearly 99.54 MPa, the increase in flexural strength was about 241%. The composites with 2 wt.%, 6 wt.%, and 8 wt.% BAR powder showed flexural strengths of 251 MPa, 293.67 MPa, and 268.33 MPa, respectively, which are about 152%, 195%, and 170% stronger than the BEC0 composite. Similarly, the highest flexural modulus was observed in the BEC4 composite, which was about 22.73 GPa. When compared with the BEC0 composite, which had a flexural modulus of nearly 13.77 GPa, the increase in flexural modulus was about 65%. This improvement in the flexural strength and moduli of the BAR-filled BEC laminates can be understood through the FTIR spectrum of the BAR powder, as shown in Figure 2. The presence of the FTIR spectrum band at 1735 cm^{-1} indicates the presence of an ester C=O bond, which is a strong and stable bond [52]. Such bonds lead to the creation of stronger interfaces with the resin and result in improved flexural properties. Also, the lignin in the BAR powder constitutes various reactive elements such as hydroxyl and methoxy groups, which were confirmed by peaks at 2919 cm^{-1} and 3347 cm^{-1} in the FTIR spectrum. Such reactive functional groups tend to bond to the epoxides of the epoxy resin, resulting in the generation of stronger interfaces. This is the reason there are published reports suggesting the use of lignin-based curing agents for epoxy resins [53]. However, the improvement in flexural strength and moduli of the BAR-filled BEC laminates follows the typical trend; the improvement is observed for the BEC2 and BEC4 laminates, and the trend reverses for the BEC6 and BEC8 laminates. This may be due to the increased viscosity of the resin at a higher wt.% addition of BAR powder. Also, due to depleting resin content at a higher wt.% loading of the BAR powder, the active functional groups of the BAR powder do not receive enough epoxide rings to react with and generate stronger interfaces. This may be the reason the flexural properties tend to decrease when BAR powder inclusion is greater than 4 wt.% in the epoxy resin.

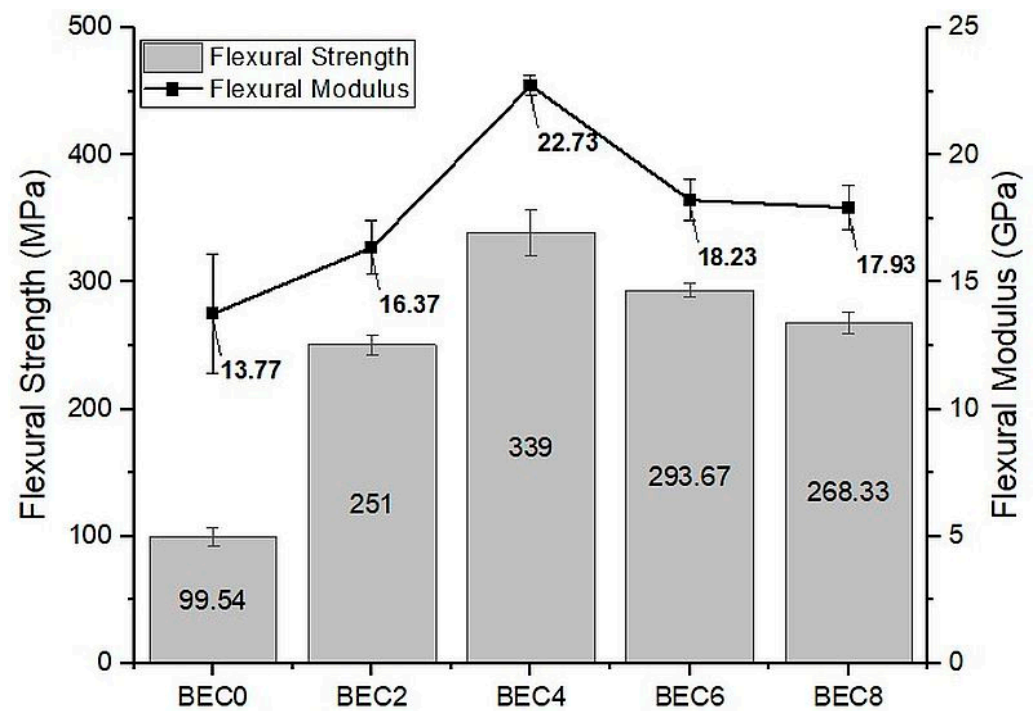


Figure 7. Flexural strength and modulus of BEC laminates.

3.3.3. Impact Strength

The results of the impact strength test are shown graphically in Figure 8. The analysis of the impact strength values indicates that the BEC laminate's ability to absorb energy before fracture increases with the addition of BAR powder. The impact strength of all BEC laminates fabricated through the inclusion of BAR powder shows an increment in comparison to the impact strength value of the unfilled BEC0 laminate. The impact strength of the BEC laminates showed an increasing trend from the BEC0 laminate to the BEC6 laminate, after which a decreasing trend was observed from the BEC6 to the BEC8 laminate. The highest impact strength was observed for the BEC6 laminate, which could absorb approximately 194.02 kJ/m^2 of energy before fracture. In comparison with the BEC0 laminate, an improvement of 44% in energy absorption was observed for the BEC6 laminate. The laminates with 2, 4, and 8 wt.% BAR powder filler absorbed nearly 177.41 kJ/m^2 , 180.62 kJ/m^2 and 191.49 kJ/m^2 respectively, which was about 32%, 34%, and 42% more than the BEC0 laminate. The improvement in the impact strength of the BEC laminates included BAR powder can be attributed to enhanced wettability of the basalt fibers with BAR-powder-infused resin, which resists fiber pull-out and the eventual delamination failing under impact loads [54]. The impact strength of a polymer composite laminate, by and large, depends upon the toughness of the matrix resin. Also, the variations in features present in different layers of the laminate due to the incorporation of fibers and fillers may give rise to different failure conditions in the intra-ply regions, which help the laminate resist delamination under impact loads [55]. Thus, for higher impact strength, it becomes more important to have better adhesion of plies through the generation of stronger interfaces. The inclusion of BAR powder in the epoxy resin resulted in enhancing the matrix toughness, which allowed the matrix to absorb more energy under impact loads. The presence of the BAR powder in the matrix increased the friction between the microfiller and the fibers, so it resisted the pull-out of the fibers. Also, the basalt fibers, which are more brittle compared to the cellulosic BAR powder [56], were coated with the BAR-powder-infused resin, which protected the fibers against impact damage.

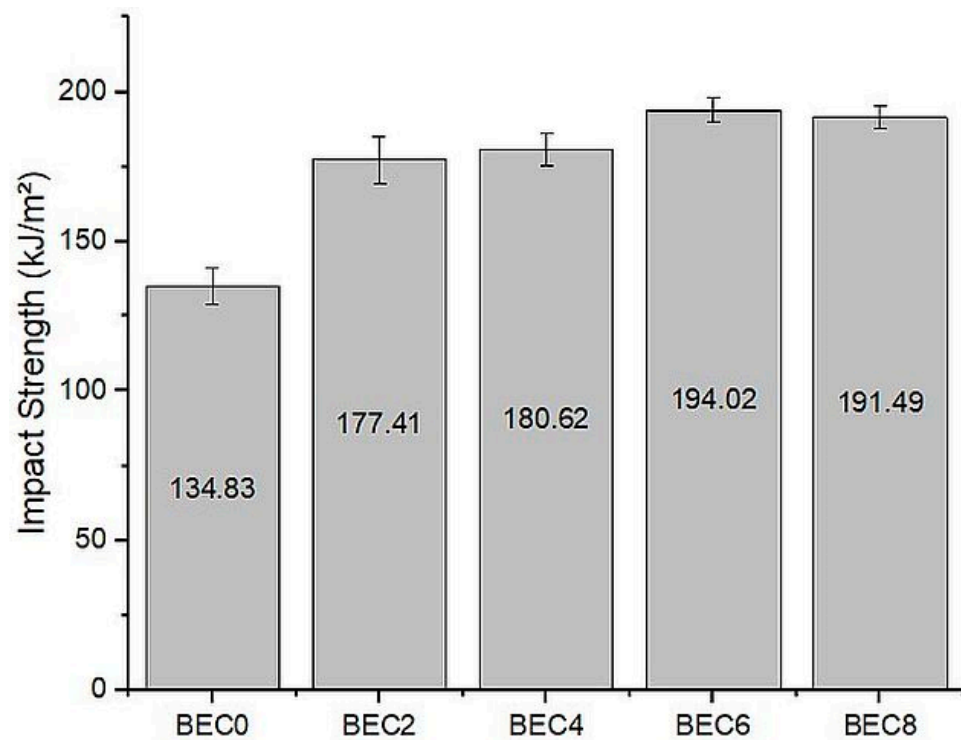


Figure 8. Impact strength of BEC laminates.

4. Morphology of BEC Laminates through SEM

A SEM analysis was carried out to further understand the failure mechanisms involved and influencing the strength of the BEC laminates. Figure 9 shows the SEM images of the fractured BEC laminates subjected to the flexural strength test. As discussed in the aforementioned paragraphs, the BEC2 and BEC4 laminates possess better mechanical properties than the BEC0, BEC6, and BEC8 laminates due to the thorough wetting of the BAR-powder-reinforced epoxy resin with the basalt fibers. The morphology of the BEC2 and BEC4 laminates shown in Figure 9a,b indicates a fractured fiber surface that was thoroughly coated with resin. Also, the fibers were held together and the fractured surface did not show any fiber pull-out. The laminate pictured in Figure 9b is characterized by the presence of fractured fibers with uneven surfaces, indicating crack deflection during fracture [57]. The indication of the presence of crack deflection also reinforces the presence of stronger and stiffer interfaces between the various components of the composite laminate. This indicates that using BAR powder as a filler strengthened the resin–fiber interface. The drop in mechanical properties of the BEC6 laminate can be understood through Figure 9c. The fractured surface of the BEC6 laminate as shown in Figure 9c indicates a widespread delamination of the plies under the applied loads. This is due to the poor adhesion of the plies with each other, indicating the lack of resin between the plies. Also, the fracture surface in Figure 9c is characterized by the presence of loose, pulled out fibers, which again can be attributed to the lack of the adhesive agent, which is the resin filled with BAR powder. As the wt.% inclusion of BAR powder increases, simultaneously, the resin content decreases. This was attributed to the decrease in the mechanical properties of the BEC8 laminate. Figure 9d shows the SEM image of the fractured surface of the BEC8 laminate, which is characterized by the presence of a huge void generated due to the deficiency of the resin.



Figure 9. SEM images of fractured BEC laminates.

5. Conclusions

BAR powder was prepared from the aerial roots of the *Ficus benghalensis* tree, popularly known as the Banyan tree. Epoxy resin was modified using the BAR powder by mixing it in different weight proportions, namely, 2%, 4%, 6%, and 8%. Basalt-fiber-reinforced composite laminates were prepared using modified resin to evaluate their mechanical properties like their tensile, flexural, and impact strengths. The results were compared with those obtained from laminates prepared with unmodified resin, i.e., with no BAR powder. The results showed significant improvement in mechanical properties with an increase in powder content, up to a certain weight proportion, beyond which the properties decreased. Though there was a decrease in the mechanical properties beyond a certain weight proportion, they were still higher than the mechanical properties of the composite prepared with unmodified resin. The highest tensile strength was obtained in the BEC4 composite, with 4% wt. BAR powder, which was 407.81 MPa, while the lowest strength among the BAR composites was obtained in the BEC8 composite, with 8% wt., which was 302.48 MPa. The tensile strength of the composite without BAR powder was found to be 251.15 MPa. Flexural strength test results followed the same trend as that of tensile strength, where the highest strength was found to be 339 MPa for the BEC4 composite, while that for the BEC0 composite was as low as 99.54 MPa. For the BEC8 composite, the strength was observed to drop to 268.33 MPa. The highest impact strength was obtained for the BEC6 composite, which showed a strength of 194.02 kJ/m², while that of the BEC0 composite

was 134.83 kJ/m². BAR powder has a high proportion of cellulose, which was found to be 52%. SEM micrographs of the flexural samples reasonably confirmed, due to the adequate wetting in BEC2 and BEC4, that these samples had relatively higher flexural strength than the others. Appreciable crack deflection was observed, indicating an improvement in stiffness due to the introduction of the BAR powder. At higher weight proportions, SEM micrographs confirmed poor resin availability between the laminates, resulting in relatively increased delamination, which was seen as one of the reasons for their poor performance when subjected to various mechanical loading stresses.

Author Contributions: Conceptualization and design of the research were conducted by S.Y.N. Experimentation was carried out by A.S.P., S.P., H.S. and J.P.J. Data curation and analysis were conducted by A.H., S.Y.N. and G.B. The original draft of the manuscript was written by A.H., and the same was reviewed by S.Y.N. and G.B. All authors have read and agreed to the published version of the manuscript.

Funding: This research received no external funding.

Data Availability Statement: Data available on request from the authors.

Acknowledgments: The authors would like to acknowledge the support rendered by the Advanced Composite Material Testing Laboratory during fabrication, the Advanced Materials Testing Laboratory during testing, and the MIT Workshops in the preparation of samples using the Abrasive Water Jet Machine.

Conflicts of Interest: The authors declare no conflict of interest.

References

1. Kumar, V.; Yadav, A. Development and Thermal Performance Evaluation of Solar Parabolic Dish Based on Fiber-Reinforced Plastic. *Heat Transf.* **2022**, *51*, 6222–6248. [[CrossRef](#)]
2. Rajak, D.K.; Wagh, P.H.; Kumar, A.; Behera, A.; Pruncu, C.I. Advanced Polymers in Aircraft Structures. In *Materials, Structures and Manufacturing for Aircraft*; Springer: Cham, Switzerland, 2022; pp. 65–88.
3. Heo, W.W.; An, S.K.; Yeum, J.H.; Yang, S.B.; Choi, S. Manufacture and Vibration-Damping Effect of Composites for Archery Carbon Fiber-Reinforced Polymer Limb with Glass Fiber-Reinforced Polymer Stabilizer. *Materials* **2023**, *16*, 4048. [[CrossRef](#)] [[PubMed](#)]
4. Guo, G.; Alam, S.; Peel, L.D. An Investigation of Deformation and Failure Mechanisms of Fiber-Reinforced Composites in Layered Composite Armor. *Compos. Struct.* **2022**, *281*, 115125. [[CrossRef](#)]
5. Demircan, G.; Ozen, M.; Kisa, M.; Acikgoz, A.; İşiker, Y. The Effect of Nano-Gelcoat on Freeze-Thaw Resistance of Glass Fiber-Reinforced Polymer Composite for Marine Applications. *Ocean Eng.* **2023**, *269*, 113589. [[CrossRef](#)]
6. Navaratnam, S.; Selvaranjan, K.; Jayasooriya, D.; Rajeev, P.; Sanjayan, J. Applications of Natural and Synthetic Fiber Reinforced Polymer in Infrastructure: A Suitability Assessment. *J. Build. Eng.* **2023**, *66*, 105835. [[CrossRef](#)]
7. Yashas Gowda, T.G.; Vinod, A.; Madhu, P.; Mavinkere Rangappa, S.; Siengchin, S.; Jawaid, M. Mechanical and Thermal Properties of Flax/Carbon/Kevlar Based Epoxy Hybrid Composites. *Polym. Compos.* **2022**, *43*, 5649–5662.
8. Selvan, M.T.G.A.; Binoj, J.S.; Moses, J.T.E.J.; Sai, N.P.; Siengchin, S.; Sanjay, M.R.; Liu, Y. Extraction and Characterization of Natural Cellulosic Fiber from Fragrant Screw Pine Prop Roots as Potential Reinforcement for Polymer Composites. *Polym. Compos.* **2022**, *43*, 320–329. [[CrossRef](#)]
9. Haris, N.I.N.; Hassan, M.Z.; Ilyas, R.A.; Suhot, M.A.; Sapuan, S.M.; Dolah, R.; Mohammad, R.; Asyraf, M.R.M. Dynamic Mechanical Properties of Natural Fiber Reinforced Hybrid Polymer Composites: A Review. *J. Mater. Res. Technol.* **2022**, *19*, 167–182. [[CrossRef](#)]
10. Khan, M.; Cao, M.; Chaopeng, X.; Ali, M. Experimental and Analytical Study of Hybrid Fiber Reinforced Concrete Prepared with Basalt Fiber under High Temperature. *Fire Mater.* **2022**, *46*, 205–226. [[CrossRef](#)]
11. Shoaib, M.; Jamshaid, H.; Alshareef, M.; Alharthi, F.A.; Ali, M.; Waqas, M. Exploring the Potential of Alternate Inorganic Fibers for Automotive Composites. *Polymers* **2022**, *14*, 4946. [[CrossRef](#)]
12. Tamás-Bényei, P.; Sántha, P. Potential Applications of Basalt Fibre Composites in Thermal Shielding. *J. Therm. Anal. Calorim.* **2023**, *148*, 271–279. [[CrossRef](#)]
13. Karacor, B.; Ozcanli, M. Thermal and Mechanical Characteristic Investigation of the Hybridization of Basalt Fiber with Aramid Fiber and Carbon Fiber. *Polym. Compos.* **2022**, *43*, 8529–8544. [[CrossRef](#)]
14. Biswas, R.; Sharma, N.; Singh, K.K. Influence of Fiber Areal Density on Mechanical Behavior of Basalt Fiber/Epoxy Composites under Varying Loading Rates: An Experimental and Statistical Approach. *Polym. Compos.* **2023**, *44*, 2222–2235. [[CrossRef](#)]
15. Yao, Y.; Wang, S.; Xu, L.; Jiang, H.; Gu, Y.; Li, G.; Cui, J. Experimental and Simulation Study on Stiffness of Basalt Fiber-Reinforced Plastic Door Interior Trimming Panel. *Arch. Civ. Mech. Eng.* **2022**, *23*, 53. [[CrossRef](#)]

16. Xiong, Z.; Lin, L.; Qiao, S.; Li, L.; Li, Y.; He, S.; Li, Z.; Liu, F.; Chen, Y. Axial Performance of Seawater Sea-Sand Concrete Columns Reinforced with Basalt Fibre-Reinforced Polymer Bars under Concentric Compressive Load. *J. Build. Eng.* **2022**, *47*, 103828. [[CrossRef](#)]
17. Karim, M.A.; Abdullah, M.Z.; Deifalla, A.F.; Azab, M.; Waqar, A. An Assessment of the Processing Parameters and Application of Fibre-Reinforced Polymers (FRPs) in the Petroleum and Natural Gas Industries: A Review. *Results Eng.* **2023**, *18*, 101091. [[CrossRef](#)]
18. Zheng, T.; Zhao, C.; He, J. Research on Fatigue Performance of Offshore Wind Turbine Blade with Basalt Fiber Bionic Plate. In *Structures*; Elsevier: Amsterdam, The Netherlands, 2023; Volume 47, pp. 466–481.
19. Liu, E. Application and Performance Discussion of Fiber-Reinforced Composite Materials in Sports Equipment Based on Image Processing Technology. *Sci. Program.* **2022**, *2022*, 6879601. [[CrossRef](#)]
20. Griffin, A.; Guo, Y.; Hu, Z.; Zhang, J.; Chen, Y.; Qiang, Z. Scalable Methods for Directional Assembly of Fillers in Polymer Composites: Creating Pathways for Improving Material Properties. *Polym. Compos.* **2022**, *43*, 5747–5766. [[CrossRef](#)]
21. Sienkiewicz, N.; Dominic, M.; Parameswaranpillai, J. Natural Fillers as Potential Modifying Agents for Epoxy Composition: A Review. *Polymers* **2022**, *14*, 265. [[CrossRef](#)] [[PubMed](#)]
22. Nazarpour-Fard, H. Rice Husk Ash: Economical and High-Quality Natural-Based Reinforcing Filler for Linear Low-Density and High-Density Polyethylene. *Polym. Renew. Resour.* **2022**, *13*, 206–222. [[CrossRef](#)]
23. Ramesh, V.; Karthik, K.; Arunkumar, K.; Unnam, N.K.; Ganesh, R.; Rajkumar, C. Effect of Sawdust Filler with Kevlar/Basalt Fiber on the Mechanical Properties Epoxy—Based Polymer Composite Materials. *Mater. Today Proc.* **2023**, *72*, 2225–2230. [[CrossRef](#)]
24. Sivakumar, V.; Kaliappan, S.; Natrayan, L.; Patil, P.P. Effects of Silane-Treated High-Content Cellulose Okra Fibre and Tamarind Kernel Powder on Mechanical, Thermal Stability and Water Absorption Behaviour of Epoxy Composites. *Silicon* **2023**, *15*, 4439–4447. [[CrossRef](#)]
25. Arivendan, A.; Thangiah, W.J.J.; Ramakrishnan, S.; Desai, D.A. Biological Waste Water Hyacinth (*Eichhornia crassipes*) Plant Powder Particle with Eggshell Filler-Reinforced Epoxy Polymer Composite Material Property Analysis. *J. Bionic Eng.* **2023**, *20*, 1386–1399. [[CrossRef](#)]
26. Coverdale Rangel Velasco, D.; Perissé Duarte Lopes, F.; Souza, D.; Colorado Lopera, H.A.; Neves Monteiro, S.; Fontes Vieira, C.M. Evaluation of Composites Reinforced by Processed and Unprocessed Coconut Husk Powder. *Polymers* **2023**, *15*, 1195. [[CrossRef](#)]
27. Hiremath, A.; Nayak, S.Y.; Heckadka, S.S.; Pramod, J.J. Mechanical Behavior of Basalt-Reinforced Epoxy Composites Modified with Biomass-Derived Seashell Powder. *Biomass Convers. Biorefinery* **2023**, 1–11. [[CrossRef](#)]
28. Felix Sahayaraj, A.; Muthukrishnan, M.; Ramesh, M. Influence of *Tamarindus indica* Seed Nano-Powder on Properties of *Luffa cylindrica* (L.) Fruit Waste Fiber Reinforced Polymer Composites. *Polym. Compos.* **2022**, *43*, 6442–6452. [[CrossRef](#)]
29. Ramesan, M.T.; Sameela, T.P.; Meera, K.; Bahuleyan, B.K.; Verma, M. In Situ Emulsion Polymerization of Poly (Vinyl Acetate) and Asparagus Racemosus Biopolymer Composites for Flexible Energy Storage Applications. *Polym. Compos.* **2023**, *44*, 4168–4177. [[CrossRef](#)]
30. Ajithram, A.; Winowlin Jappes, J.T.; Rajini, N.; Siva, I.; Sumesh, K.R.; Dawood, D. Serious Ecological Threat Water Hyacinth (*Eichhornia crassipes*) Plant into Successive Hyacinth Ash with Eggshell Filler Reinforced Polymer Composite—Waste into Zero Waste Concept. *Proc. Inst. Mech. Eng. Part E J. Process Mech. Eng.* **2023**. [[CrossRef](#)]
31. Khuntia, T.; Biswas, S. Mechanical, Viscoelastic, and Flammability Properties of Polymer Composites Reinforced with Novel Sirisha Bark Filler. *J. Ind. Text.* **2022**, *51*, 5887S–5909S. [[CrossRef](#)]
32. Rajamanikandan, T.; Banumathi, S.; Karthikeyan, B.; Palanisamy, R.; Bajaj, M.; Zawbaa, H.M.; Kamel, S. Investigation of Dielectric and Mechanical Properties of Lignocellulosic Rice Husk Fibril for High and Medium Voltage Electrical Insulation Applications. *J. Mater. Res. Technol.* **2023**, *22*, 865–878. [[CrossRef](#)]
33. Ayyanar, C.B.; Dharshinii, M.D.; Marimuthu, K.; Akhil, S.; Mugilan, T.; Bharathiraj, C.; Mavinkere Rangappa, S.; Khan, A.; Siengchin, S. Design, Fabrication, and Characterization of Natural Fillers Loaded HDPE Composites for Domestic Applications. *Polym. Compos.* **2022**, *43*, 5168–5178. [[CrossRef](#)]
34. Rana, P.; Chopra, S. Extraction and Characterization of Inherently Antimicrobial Fibres from Aerial Roots of Banyan Tree. *J. Nat. Fibers* **2022**, *19*, 6196–6213. [[CrossRef](#)]
35. Ganapathy, T.; Sathiskumar, R.; Senthamaraiannan, P.; Saravanakumar, S.S.; Khan, A. Characterization of Raw and Alkali Treated New Natural Cellulosic Fibres Extracted from the Aerial Roots of Banyan Tree. *Int. J. Biol. Macromol.* **2019**, *138*, 573–581. [[CrossRef](#)]
36. Mohan, S.J.; Devasahayam, P.S.S.; Suyambulingam, I.; Siengchin, S. Suitability Characterization of Novel Cellulosic Plant Fiber from *Ficus Benjamina* L. Aerial Root for a Potential Polymeric Composite Reinforcement. *Polym. Compos.* **2022**, *43*, 9012–9026. [[CrossRef](#)]
37. Ganapathy, T.; Sathiskumar, R.; Sanjay, M.R.; Senthamaraiannan, P.; Saravanakumar, S.S.; Parameswaranpillai, J.; Siengchin, S. Effect of Graphene Powder on Banyan Aerial Root Fibers Reinforced Epoxy Composites. *J. Nat. Fibers* **2021**, *18*, 1029–1036. [[CrossRef](#)]
38. Ganapathy, T.; Ramasamy, K.; Suyambulingam, I.; Siengchin, S. Synergetic Effect of Graphene Particles on Novel Biomass—Based *Ficus Benghalensis* Aerial Root/Flax Fiber—Reinforced Hybrid Epoxy Composites for Structural Application. *Biomass Convers. Biorefinery* **2023**, 1–38. [[CrossRef](#)]

39. Chen, X.; Zhang, Y.; Huo, H.; Wu, Z. Study of High Tensile Strength of Natural Continuous Basalt Fibers. *J. Nat. Fibers* **2020**, *17*, 214–222. [[CrossRef](#)]
40. Heckadka, S.S.; Nayak, S.Y.; Samant, R. Mangifera Indica Mid-Rib Fibers as Reinforcements for CNSL-Epoxy Composites. *J. Text. Inst.* **2022**, *113*, 657–670. [[CrossRef](#)]
41. Nagarjun, J.; Kanchana, J.; RajeshKumar, G.; Manimaran, S.; Krishnaprakash, M. Enhancement of Mechanical Behavior of PLA Matrix Using Tamarind and Date Seed Micro Fillers. *J. Nat. Fibers* **2022**, *19*, 4662–4674. [[CrossRef](#)]
42. Joshi, S.; Hiremath, A.; Nayak, S.Y.; Jaideep, J.P.; Thipperudrappa, S. Hybridization Effect on the Mechanical Properties of Basalt Fiber Reinforced ZnO Modified Epoxy Composites. *Polym. Compos.* **2022**, *43*, 5704–5714. [[CrossRef](#)]
43. Iyer, T.; Nayak, S.Y.; Hiremath, A.; Heckadka, S.S.; Jaideep, J.P. Influence of TiO₂ Nanoparticle Modification on the Mechanical Properties of Basalt-Reinforced Epoxy Composites. *Cogent Eng.* **2023**, *10*, 2227397. [[CrossRef](#)]
44. Thipperudrappa, S.; Ullal Kini, A.; Hiremath, A. Influence of Zinc Oxide Nanoparticles on the Mechanical and Thermal Responses of Glass Fiber-Reinforced Epoxy Nanocomposites. *Polym. Compos.* **2020**, *41*, 174–181. [[CrossRef](#)]
45. Nayak, S.Y.; Satish, S.B.; Sultan, M.T.H.; Kini, C.R.; Shenoy, K.R.; Samant, R.; Sarvade, P.P.; Basri, A.A.; Mustapha, F. Influence of Fabric Orientation and Compression Factor on the Mechanical Properties of 3D E-Glass Reinforced Epoxy Composites. *J. Mater. Res. Technol.* **2020**, *9*, 8517–8527. [[CrossRef](#)]
46. Santos, J.I.; Martín-Sampedro, R.; Fillat, Ú.; Oliva, J.M.; Negro, M.J.; Ballesteros, M.; Eugenio, M.E.; Ibarra, D. Evaluating Lignin-Rich Residues from Biochemical Ethanol Production of Wheat Straw and Olive Tree Pruning by FTIR and 2d-Nmr. *Int. J. Polym. Sci.* **2015**, *2015*, 314891. [[CrossRef](#)]
47. Yang, H.; Yan, R.; Chen, H.; Lee, D.H.; Zheng, C. Characteristics of Hemicellulose, Cellulose and Lignin Pyrolysis. *Fuel* **2007**, *86*, 1781–1788. [[CrossRef](#)]
48. Szymanska-Chargot, M.; Zdunek, A. Use of FT-IR Spectra and PCA to the Bulk Characterization of Cell Wall Residues of Fruits and Vegetables Along a Fraction Process. *Food Biophys.* **2013**, *8*, 29–42. [[CrossRef](#)]
49. Sun, S.N.; Yuan, T.Q.; Li, M.F.; Cao, X.F.; Xu, F.; Liu, Q.Y. Structural Characterization of Hemicelluloses from Bamboo Culms (*Neosinocalamus affinis*). *Cellul. Chem. Technol.* **2012**, *46*, 165–176.
50. Nikolic, G.; Zlatkovic, S.; Cakic, M.; Cakic, S.; Lacnjevac, C.; Rajic, Z. Fast Fourier Transform IR Characterization of Epoxy GY Systems Crosslinked with Aliphatic and Cycloaliphatic EH Polyamine Adducts. *Sensors* **2010**, *10*, 684–696. [[CrossRef](#)]
51. Chen, C.; Zhu, M.; Li, M.; Fan, Y.; Sun, R.-C. Epoxidation and Etherification of Alkaline Lignin to Prepare Water-Soluble Derivatives and Its Performance in Improvement of Enzymatic Hydrolysis Efficiency. *Biotechnol. Biofuels* **2016**, *9*, 87. [[CrossRef](#)]
52. Cho, B.-G.; Joshi, S.R.; Lee, J.; Park, Y.-B.; Kim, G.-H. Direct Growth of Thermally Reduced Graphene Oxide on Carbon Fiber for Enhanced Mechanical Strength. *Compos. Part B Eng.* **2020**, *193*, 108010. [[CrossRef](#)]
53. Chen, B.; Zhang, Q.; Lu, M.; Meng, H.; Qu, Z.; Xu, C.; Jiao, E. Synthesis of a Novel Lignin-Based Epoxy Resin Curing Agent and Study of Cure Kinetics, Thermal, and Mechanical Properties. *J. Appl. Polym. Sci.* **2021**, *138*, 50523. [[CrossRef](#)]
54. Taghipoor, H.; Fereidoon, A.; Ghasemi-Ghalebahman, A.; Mirzaei, J. Experimental Assessment of Mechanical Behavior of Basalt/Graphene/PP-g-MA-Reinforced Polymer Nanocomposites by Response Surface Methodology. *Polym. Bull.* **2023**, *80*, 7663–7685. [[CrossRef](#)]
55. Hemath, M.; Mavinkere Rangappa, S.; Kushvaha, V.; Dhakal, H.N.; Siengchin, S. A Comprehensive Review on Mechanical, Electromagnetic Radiation Shielding, and Thermal Conductivity of Fibers/Inorganic Fillers Reinforced Hybrid Polymer Composites. *Polym. Compos.* **2020**, *41*, 3940–3965. [[CrossRef](#)]
56. Sergi, C.; Sbardella, F.; Lilli, M.; Tirillò, J.; Calzolari, A.; Sarasini, F. Hybrid Cellulose–Basalt Polypropylene Composites with Enhanced Compatibility: The Role of Coupling Agent. *Molecules* **2020**, *25*, 4384. [[CrossRef](#)]
57. Nagi, C.S.; Ogin, S.L.; Mohagheghian, I.; Crean, C.; Foreman, A.D. Spray Deposition of Graphene Nano-Platelets for Modifying Interleaves in Carbon Fibre Reinforced Polymer Laminates. *Mater. Des.* **2020**, *193*, 108831. [[CrossRef](#)]

Disclaimer/Publisher’s Note: The statements, opinions and data contained in all publications are solely those of the individual author(s) and contributor(s) and not of MDPI and/or the editor(s). MDPI and/or the editor(s) disclaim responsibility for any injury to people or property resulting from any ideas, methods, instructions or products referred to in the content.